Available online at www.sciencedirect.com
SCIENCE DIRECT®
Polymer 45 (2004) 2393–2401
polymer
www.elsevier.com/locate/polymer

Effects of talc orientation and non-isothermal crystallization rate on crystal orientation of polypropylene in injection-molded polypropylene/ethylene–propylene rubber/talc blends

Woo Jin Choi, Sung Chul Kim*

Center for Advanced Functional Polymers, Korea Advanced Institute of Science and Technology, 373-1 Guseong-dong, Yuseong-gu, Daejeon 305-701, South Korea

Received 28 May 2003; received in revised form 1 January 2004; accepted 30 January 2004

Abstract

The effects of talc orientation and non-isothermal crystallization rate on the crystal orientation of polypropylene in the injection-molded PP/EPR/Talc blends were studied by using AFM, DSC, SEM and XRD. Polypropylene was transcrystallized on the talc surface and the polypropylene crystal was oriented perpendicular to the talc surface. Therefore, the crystal orientation was affected by the talc orientation. At the surface of injection-molded specimens, the crystal orientation increased with decreasing the molecular weight of EPRs and increasing the talc content. Because talc particles were nearly oriented parallel to the flow direction in the skin layer of the specimens, the crystal orientation was amplified by the increased crystallization rate. The non-isothermal crystallization behavior of PP/EPR/Talc blends was investigated in terms of the molecular weight of EPRs and the talc content. Non-isothermal crystallization rate increased with decreasing the molecular weight of EPRs due to the plasticizing effect of EPRs and increasing the content of talc which acts as nucleating agent.

Keywords: Non-isothermal crystallization; Polypropylene crystal orientation; Talc orientation

1. Introduction

Polypropylene is one of the important commodity polymers. The application of polypropylene in automobiles, household appliances and the construction industry requires stiffness and toughness similar to those of engineering plastics. The application of polypropylene, however, has been limited by its high flammability, tendency to brittleness at temperatures below its glass transition temperature and low stiffness particularly at elevated temperatures. In order to overcome these limitations, numerous studies have been carried out to improve the toughness, stiffness, and strength balance; polypropylene has been modified by many fillers and elastomers. PP/filler composites and PP/elastomer blends exhibit either increased stiffness or improved fracture toughness. Recently, polypropylene has been incorporated both by elastomers and by rigid fillers to be both stiffer and tougher than the neat polypropylene.

Nomura et al. reported the crystal orientation of polypropylene in PP/EPR blends [1] and PP/EPR/Talc blends [2]. Obata et al. [3] also reported the crystal orientation in PP/EPR/Talc blends.

Many researchers studied the crystal orientation, the crystal structure and the crystalline morphology of polypropylene in talc-filled polypropylene [4–12]. Naiki et al. [13] reported that polypropylene could be transcrystallized on the cleavage surface of talc and the polypropylene crystal was oriented perpendicular to the surface of talc.

Though there are many studies on the crystal orientation in injection-molded talc-filled PP and PP/EPR/Talc blends, there have been a few studies on the factors which affect the degree of crystal orientation.

In the present work, we investigated the crystalline morphology of polypropylene by using an AFM and the relationship between the crystal orientation of polypropylene and the talc orientation in PP/EPR/Talc blends. The effects of the molecular weight of EPRs and the talc content on non-isothermal crystallization rate which could amplify the degree of the crystal orientation of polypropylene in PP/EPR/Talc blends were also investigated.

* Corresponding author. Tel.: +82-42-869-3914; fax: +82-42-869-8435.
E-mail address: kimsc@kaist.ac.kr (S.C. Kim).

0032-3861/$ - see front matter © 2004 Elsevier Ltd. All rights reserved.
doi:10.1016/j.polymer.2004.01.058

Table 1
Characteristics of PP and EPRs

Grade		$\bar{M}_n$	$\bar{M}_w$	PDI	MI (g/10 min)	Propylene content
PP	HI-700X	40,000	249,200	6.23	22	–
EPR	P-0180	68,500	124,900	1.82	8.1	26 wt%
	P-0280	74,500	139,800	1.88	5.4	26 wt%
	P-0480	92,300	194,300	2.11	1.8	26 wt%

2. Experimental

2.1. Materials

As matrix polymer, homo-isotactic polypropylene HI-700X (Samsung General Chemicals, Korea) was used, while P-0180, P-0280, and P-0480 (Mitsui Chemical Co., Ltd., Japan) were used as elastomer (EPR) components; talc (average diameter = 5.69 μm, average aspect ratio = 6.62) was used as the filler. The characteristics of the resins are shown in Table 1.

2.2. Sample preparation

Polypropylene pellets were mixed with the fixed amount of the elastomers and talc; then extruded by using a counter-rotating twin-screw exturder Brabender DSK42/7 in which temperature profile was 170–205–220–215 °C and screw velocity was 60 rpm. The extudates were cut into pellets, the pellets were then injected by using an injection-molding machine of Newbery HV1-25RS. The temperature profile was 210–220–230 °C and the injection pressure was 12.4 MPa. The mold temperature was 50 °C. The dimension of the injection-molded specimens was $60 \times 10 \times 3$ mm^3. Sample notation and the composition of blends are shown in Table 2.

2.3. AFM measurement

Samples of AFM measurement were prepared by cutting the injection-molded specimens using a RMC MT-7000 microtome with CR-21 cryogenic system. Glass knives were used at temperature of −90 to −70 °C, while the temperature of the specimens was −120 to −100 °C.

Table 2
Sample notation and the composition of blends

Blend	PP (HI-700X) (wt%)	EPR (wt%)			Talc (wt%)	Mold temperature (°C)
		P-0180	P-0280	P-0480		
L-10	60	30	–	–	10	50
M-10	60	–	30	–	10	50
H-10	60	–	–	30	10	50
L-05	63.33	31.67	–	–	5	50
L-20	53.33	26.67	–	–	20	50

In order to study the crystalline morphology of PP/EPR/Talc blends by using an AFM, the crystalline structure must be exposed to the AFM probe tip. This was achieved by removing the top amorphous layer of microtomed samples with a permanganic etchant as follows [14]: the microtomed samples were immersed for 5–7 h at room temperature in a permanganic etchant. The permanganic etchant consisted of 0.7% w/v of potassium permanganate ($KMnO_4$) in a mixture of sulfuric acid (H_2SO_4) and phosphoric acid (H_3PO_4) in the volumetric ratio of 2:1. The etched samples were washed with a diluted sulfuric acid at the volumetric ratio of 2:7 in distilled water. The samples were then washed with 35% hydrogen peroxide to remove residual manganese dioxide or permanganate. The final step was to wash the samples with distilled water, and finally with acetone. They were dried in a vacuum oven.

AFM images were obtained by using a Digital Instruments Nanoscope IIIa in the Tapping™ mode with the standard etched silicon probe tips. The scanning frequency was 0.3 Hz and scanner was type 'E'. All the images shown here are 'Height' images and have been filtered through the 'Planefit' procedure.

2.4. Structural analysis

2θ-scan X-ray diffraction curves were measured at the central of the injection-molded specimen with a Rigaku X-ray diffractometer D/MAX III-C. The sample was abraded to obtain the WAXD patterns as a function of the depth and the pattern of the surface was measured without any abrasion. Using a goniometer, 2θ scans were carried out at a scan speed of 4°/min from 5 to 35°. In order to evaluate the degree of crystal orientation, the ratio of the intensity of the (040) reflection ($2\theta = 14.1°$), $I(040)$, and the (110) reflection ($2\theta = 16.9°$), $I(110)$ was used. For isotropic PP crystal, the relative intensity $I(040)/I(110)$ lies in the range 0.667–0.769 [4].

2.5. Measurement of talc orientation

Because of disk-shaped talc particles and flow profile in injection-molding, the edge of talc particles was shown in SEM images as shown in Fig. 1 and the talc orientation could be calculated by the angle of the talc direction to the flow direction. The angle between the talc direction and the flow direction was obtained from SEM images (scan range was about 100×60 μm) of the side view along the depth by

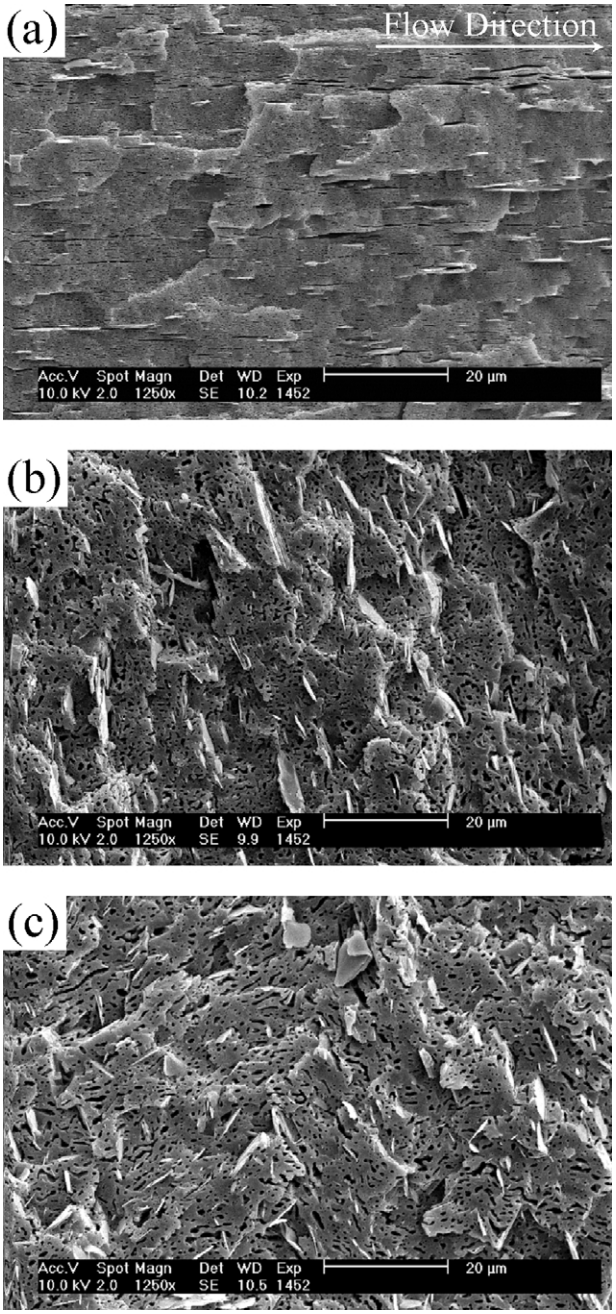

Fig. 1. SEM Images of the side view along the depth. (a) Depth: 0.3 mm, $f = 0.99$; (b) depth: 1.0 mm, $f = -0.23$; (c) depth: 2.0 mm, $f = 0.03$.

using a Leica Qwin Image processing and analysis software. The talc orientation was quantified by the Hermans orientation function f as follows [15]:

$$f = \frac{3\langle\cos^2\theta\rangle - 1}{2}$$

where θ represents the angle between the direction of talc particles and the flow direction. Hermans orientation function f takes value 1 when talc particles are completely oriented parallel to the flow direction, 0 for the case of random orientation and -0.5 for the case of complete orientation perpendicular to the flow direction as shown in Fig. 2.

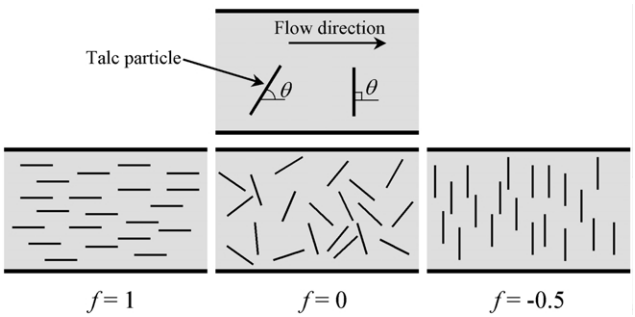

Fig. 2. Illustrations of talc orientation for the three values of the Hermans orientation function (f) -0.5, 0 and 1.

2.6. Glass transition temperature measurement

The glass transition temperatures of polypropylene, EPRs, and blends were measured by using a Rheometric Scientific DMTA IV in dual-cantilever bending mode. The measurements were made at a fixed frequency of 1 Hz with a heating rate of 3 °C/min over a temperature range of -100–80 °C.

2.7. Non-isothermal crystallization analysis

Non-isothermal crystallization analysis was performed by using a TA Instruments DSC 2010 with a liquid nitrogen cooling accessory (LNCA). Samples for DSC experiments were prepared by using a Brabender W50H mixer. The mixing was carried out for 10 min at 210 °C and the rotor velocity was 30 rpm. The samples had the same composition as the injection-molded specimens had. The following measurement procedure was applied.

The samples were heated up to 210 °C and held there for 15 min in order to eliminate small residual nuclei. The melt samples were cooled to crystallize at a selected cooling rate. The cooling rates were 2, 5, 8, 10, 12 and 14 °C/min. Sample weights were 6–13 mg. All operations were carried out under a nitrogen purge.

3. Results and discussion

3.1. Crystalline morphology of polypropylene in PP/EPR/Talc blends

To determine the effect of talc on the orientation of polypropylene crystal in PP/EPR/Talc blends, the crystalline morphology of the blends was investigated by using an AFM. Fig. 3 shows the AFM images of the edge view in the skin layer of L-10. In the AFM images, talc was oriented parallel to the surface of specimen and the flow direction; the polypropylene lamellae were arranged perpendicular to the cleavage surface of talc due to the transcrystallization of

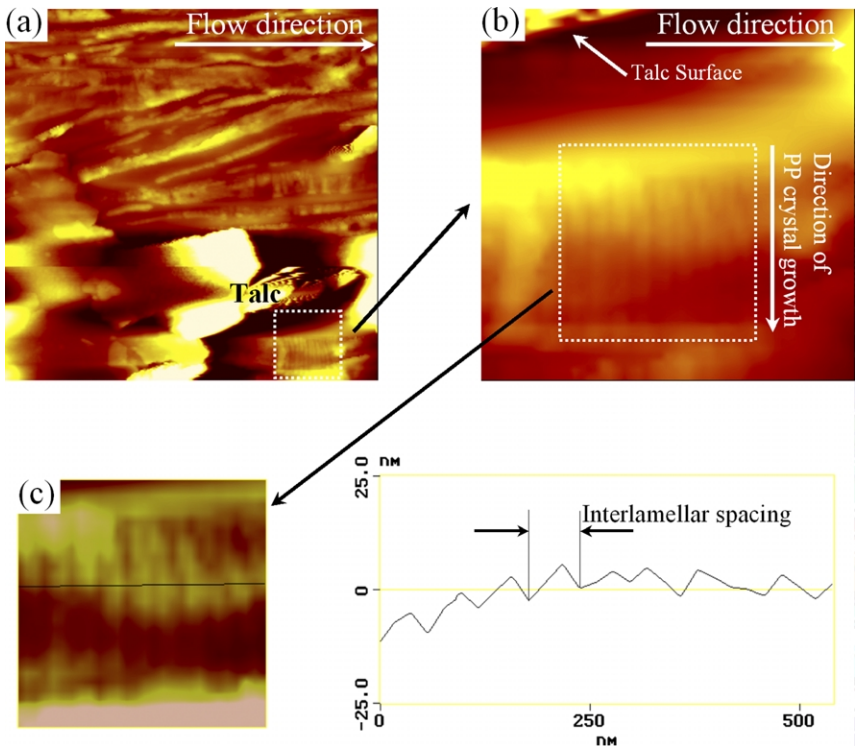

Fig. 3. AFM images of the skin layer of the microtomed L-10. (a) 5 × 5 μm, *z*-range = 300 nm; (b) 1.04 × 1.04 μm, *z*-range = 400 nm; (c) 2D-section of the image along an axis perpendicular to the lamellae orientation.

polypropylene. This result agrees with previous results that polypropylene is transcrystallized on the talc surface [13]. The lamellar thickness can be deduced from the measurement of the interlamellar distances which can be obtained through a 2D-sectional analysis [16]. Because the width of the lamellar peak depends strongly on both the acid attack in the procedure of permanganic etching and the tip convolution, it is less accurate that the lamellar thickness is directly obtained by the measurement of the half-height width of the lamellar peak. Therefore, the interlamellar spacing was measured instead of the half-height width of the lamellar peak. The mean-averaged value of the interlamellar distance was found to be 50 ± 11 nm.

3.2. Crystal orientation with varying the talc orientation

Generally, the type of flow affects the orientation of anisotropic fillers such as fiber, mica, and talc in an injection-molding. Because the talc has disc-shape, the talc orientation depends on the type of flow. In a simple shear flow, anisotropic fillers are nearly parallel to the flow lines. Vincent and Agassant reported the correlation between experimental study and calculations of the orientation of short glass fiber in an injection-molding process [17]. Their numerical computation shows that shear rate reaches a maximum near the mold wall, whereas the elongation rate reaches maximum at the center of the mold. It also shows that the shear rate is nearly a hundred times greater than the elongational rate. Thus, the combination of this flow pattern and the microrheological calculations of the particle motion explained the experimentally observed orientation of short glass fibers and the difference between skin and core orientation. In the skin, the shear flow is predominant and it orients the fibers in the flow direction. In the core, either negative or positive elongational flow is predominant and it orients the fibers perpendicular or parallel to the flow direction, respectively. Because the talc is anisotropic filler, the orientation of talc will be similar to that of glass fiber.

The plots of crystal orientation and talc orientation along depth of L-10 are shown in Fig. 4. In the core (depth: 1.0–2.0 mm), the talc particles were nearly oriented perpendicular to the flow direction ($f \approx -0.5$) or they were randomly oriented ($f \approx 0$); the crystal orientation showed lower value ($I(040)/I(110) \approx 0.5$–$2.1$). In the skin (depth: 0.0–0.5 and 2.5–3.0 mm), the talc was nearly oriented parallel to the flow direction ($f > 0.95$) and the degree of crystal orientation showed high value ($I(040)/I(110) \approx 10.6$–$41.0$). The tendencies of the talc orientation and crystal orientation were similar to each other. That is, the talc orientation strongly affects the crystal orientation because polypropylene is transcrystallized on the cleavage surface of talc and PP crystal grows perpendicular to the talc surface. Therefore, the degree of the crystal orientation increased with the talc orientation.

3.3. Non-isothermal crystallization kinetics

Figs. 5 and 6 show the degree of crystal orientation with

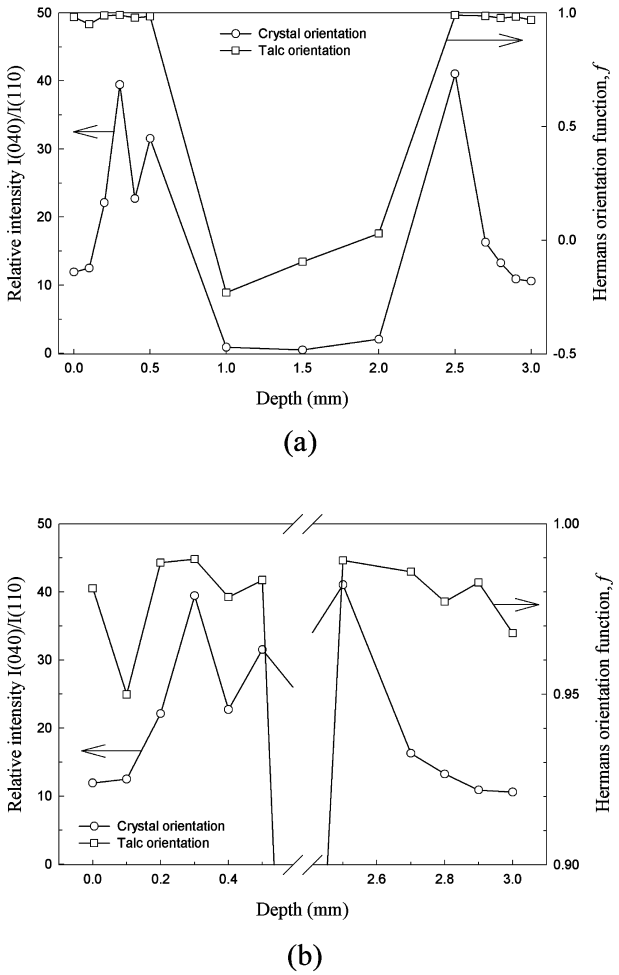

Fig. 4. Crystal orientation and talc orientation along the depth for L-10. (a) Whole specimen, 0.0–3.0 mm; (b) along the surface, 0.0–0.5 and 2.5–3.0 mm.

the varying molecular weight of EPR and the talc content on the surface of PP/EPR/Talc blends (depth: 0.0 mm), respectively. The degree of crystal orientation increased with decreasing the molecular weight of EPRs and with increasing the talc content. Because talc particles were nearly oriented parallel to the flow direction, the crystal orientation may be amplified by the crystallization rate. The non-isothermal crystallization rate was investigated since the injection-molded specimens were crystallized in non-isothermal condition.

Two non-isothermal crystallization kinetic equations are applied to investigate the non-isothermal crystallization: The Ozawa equation [18] and the combined equation [19] of the Avrami equation and the Ozawa equation.

As the non-isothermal crystallization was a rate dependent process, Ozawa has extended the Avrami equation for isothermal crystallization to non-isothermal crystallization at a controlled constant cooling rate from a molten state by replacing t in Avrami equation with T/C, as follows:

$$1 - X_T = \exp\left(-\frac{K^*(T)}{C^m}\right) \tag{1}$$

where X_T is the relative crystallinity, $K^*(T)$, the cooling function, C, the cooling rate, and m is the Ozawa exponent which depends on the crystal growth and nucleation mechanism. The cooling function, $K^*(T)$, is similar to the growth rate constant of the Avrami equation in physical meaning. The following equation has been derived by double logarithm of Eq. (1) and rearrangement:

$$\log[-\ln(1 - X_T)] = \log K^*(T) - m \log C \tag{2}$$

Plotting $\log[-\ln(1 - X_T)]$ versus $\log C$ at a given temperature, if the Ozawa equation is valid, a series of straight lines

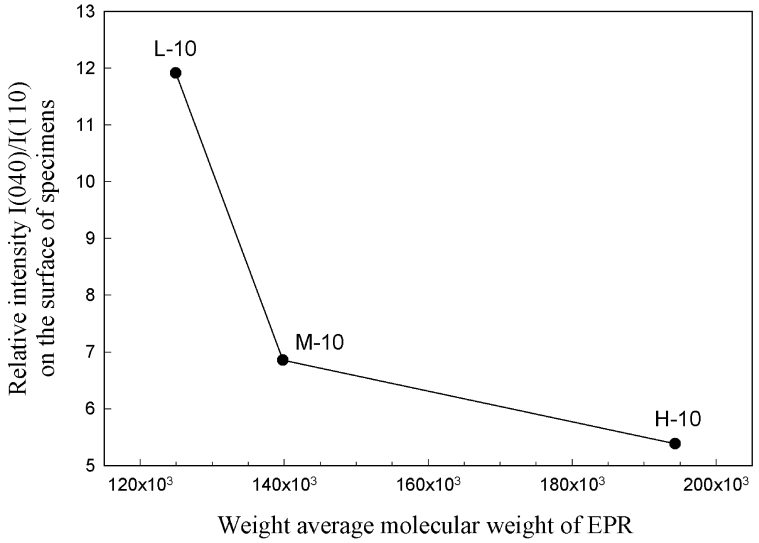

Fig. 5. Degree of crystal orientation versus weight average molecular weight of EPRs.

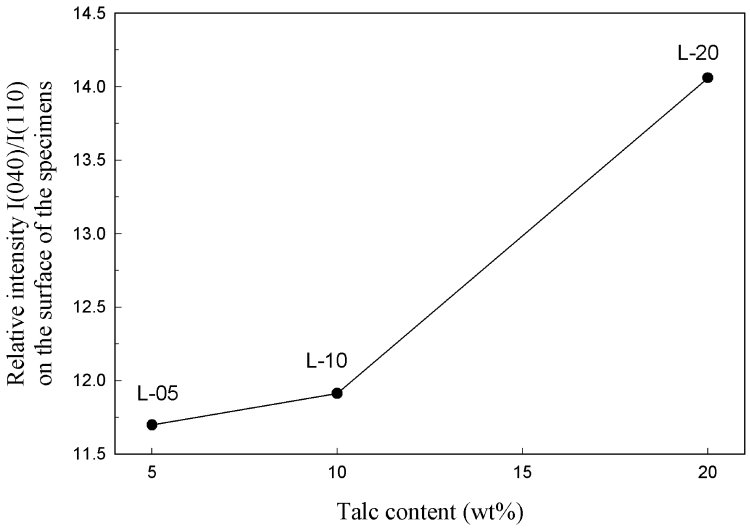

Fig. 6. Degree of crystal orientation with talc content.

should be obtained, and then $K^*(T)$ and m can be obtained from the intercept and slope, respectively.

Figs. 7 and 8 show the plot of the cooling function versus crystallization temperature for L-10, M-10 and H-10; L-05, L-10 and L-20, respectively. The cooling function increased with decreasing the molecular weight of EPRs below 131 °C in Fig. 7 and with increasing talc content above 125 °C in Fig. 8. The results from Figs. 7 and 8 can be explained by the plasticizing effect of EPRs on polypropylene and the effect of talc as nucleating agent, respectively. Generally, crystallization can be divided into two mechanisms: nucleation and growth. At high temperature, crystallization is controlled by the nucleation; at low temperature, crystal growth is the controlling factor for overall crystallization.

In L-10, M-10 and H-10, the molecular weight was different to each other, whereas the talc content was the same. Table 3 shows the glass transition temperatures for PP, EPRs and the blends. The glass transition temperature of PP-rich phase decreased with decreasing the molecular weight of EPRs. It means that the EPR with low molecular weight shows higher plasticizing effect, which can affect the growth rate at low temperature. Therefore, there was significant difference of the cooling function below 131 °C. However, the cooling functions for L-10, M-10 and H-10 were almost the same at temperature above 131 °C, since in this temperature range, the overall crystallization is controlled by the nucleation and all three samples have the same talc content.

In L-05, L-10 and L-20, the EPR with low molecular weight was used with varying the concentration of talc. The effect of talc concentration on the overall crystallization becomes significant in the temperature range above 125 °C where the overall crystallization is nucleation-control.

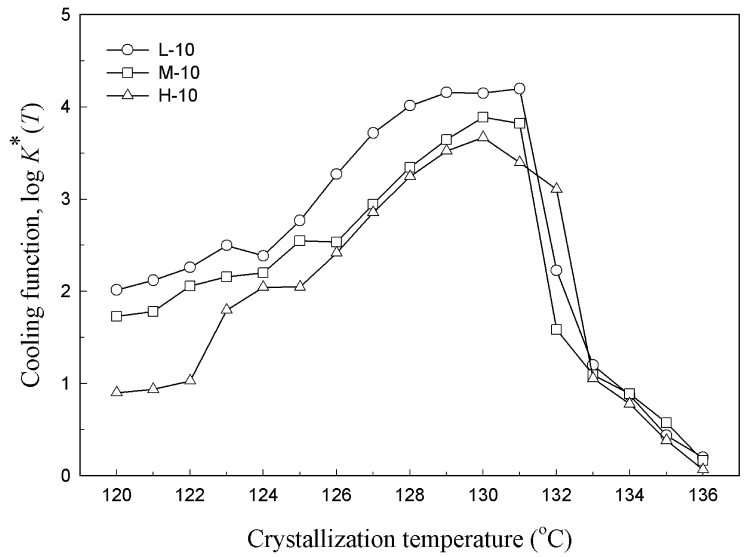

Fig. 7. Variations of cooling function versus crystallization temperature for L-10, M-10 and H-10.

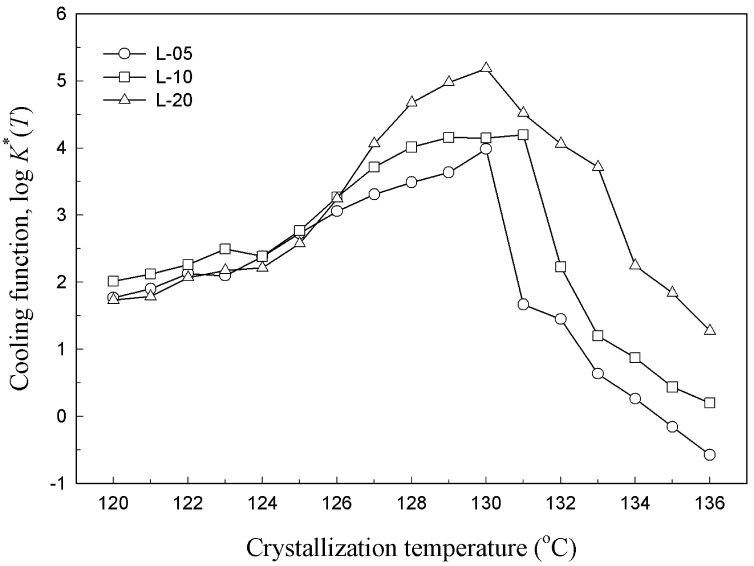

Fig. 8. Variations of cooling function versus crystallization temperature for L-05, L-10 and L-20.

Liu et al. proposed a convenient equation for non-isothermal crystallization derived by combining the Avrami equation with the Ozawa equation [19]. Under non-isothermal conditions, the crystallinity is related to both the cooling rate C and the crystallization time t. At a fixed crystallinity, the relationship between C and t can be derived by combining the Avrami equation (Eq. (3)) and the Ozawa equation (Eq. (2)) as follows:

$$\log[-\ln(1 - X_T)] = \log K + n \log t \tag{3}$$

where K is the growth rate constant, X_T is the relative crystallinity and n is the Avrami exponent.

Combining Eqs. (2) and (3):

$$\log K + n \log t = \log K^*(T) - m \log C \tag{4}$$

Following equation can be derived by the rearrangement of Eq. (4):

$$\log C = \log F(T) - a \log t \tag{5}$$

where the parameter $F(T) = [K^*(T)/K]^{1/m}$ refers to the value of cooling rate, which has to be chosen at a unit crystallization time when the measured system amounts to a certain degree of crystallinity; a is the ratio of the Avrami exponent n to the Ozawa exponent m, i.e. $a = n/m$. A lower $F(T)$ means a higher crystallization rate. In Figs. 9 and 10, the kinetic parameter $F(T)$ decreased with decreasing the molecular weight of EPRs and with increasing the talc content, respectively. Therefore, the crystallization rate increased with decreasing the molecular weight of EPRs and with increasing the talc content. These results had the same tendency with the results from Ozawa equation.

4. Conclusions

In this study, the crystalline morphology, the relationship between the crystal orientation and the talc orientation, and the effect of the non-isothermal crystallization rate on the crystal orientation in the skin layer were investigated. The non-isothermal crystallization rate was investigated in terms of the molecular weight of EPRs and the talc content.

Polypropylene was transcrystallized on the talc surface

Table 3
Glass transition temperature and T_g-shift for PP, EPR and blends

	$T_{g,\text{EPR-rich phase}}$	$\Delta T_{g,\text{EPR-rich phase}}$	$T_{g,\text{PP-rich phase}}$	$\Delta T_{g,\text{PP-rich phase}}$
PP(HI-700X)	–	–	19.202[a]	–
P-0180	−32.829[b]	–	–	–
P-0280	−32.901[b]	–	–	–
P-0480	−32.874[b]	–	–	–
L-10	−32.871	0.003	15.288	−3.914
M-10	−33.284	−0.383	15.640	−3.562
H-10	−32.089	0.740	16.899	−2.305

[a] Glass transition temperature for PP.
[b] Glass transition temperature for EPRs.

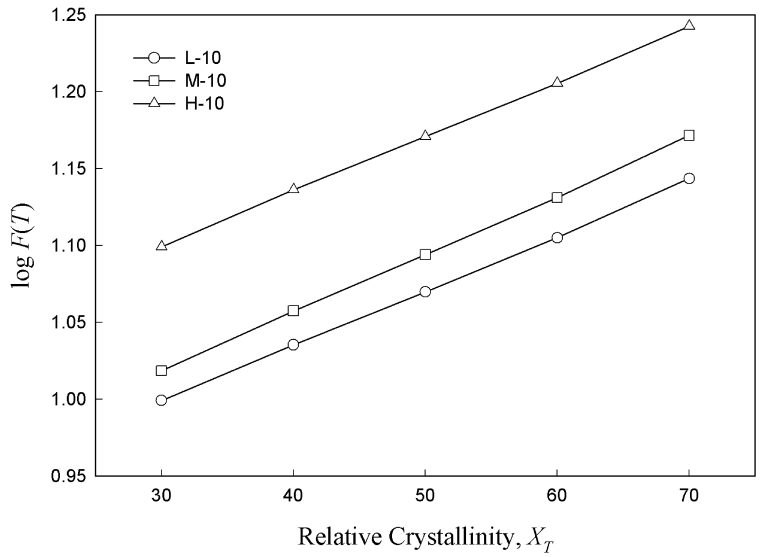

Fig. 9. Plots of log $F(T)$ versus relative crystallinity for L-10, M-10 and H-10.

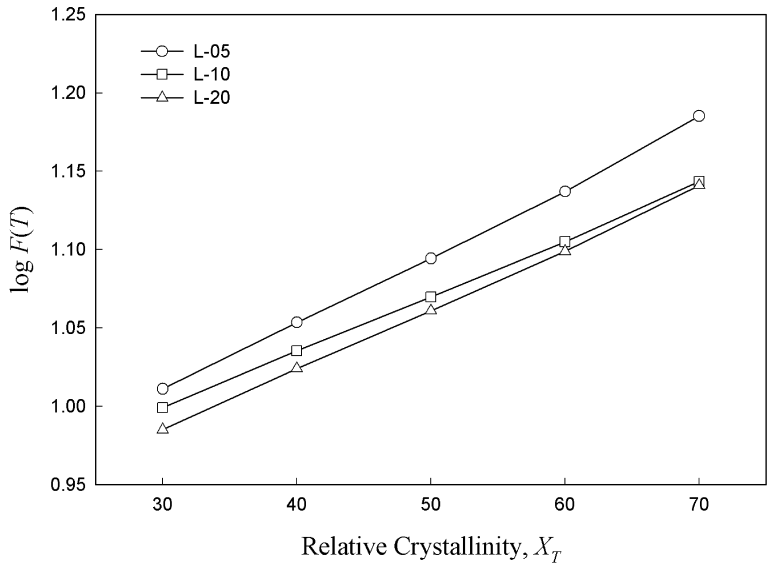

Fig. 10. Plots of log $F(T)$ versus relative crystallinity for L-05, L-10 and L-20.

and oriented perpendicular to the talc surface. Its interlamellar distance was measured to be 50 ± 11 nm by using an AFM.

In the skin layer of injection-molded specimen, talc particles were oriented parallel to the flow direction ($f >$ 0.95), so the crystal orientation showed higher value. In the core layer, however, talc was oriented either randomly or perpendicular to the flow direction ($f \approx 0 - -0.5$), so the degree of the crystal orientation showed lower value. These phenomena resulted from the transcrystallization of polypropylene on the talc surface and the talc orientation during injection-molding process.

The degree of crystal orientation can be amplified by the crystallization rate. The crystal orientation increased with decreasing the molecular weight of EPRs and increasing the talc content. As the molecular weight of EPRs decreased, the crystallization rate increased due to the plasticizing effect, while the crystallization rate increased with increasing talc content that acts as nucleating agent.

Acknowledgements

The authors acknowledge the financial support of Honam Petrochemical Corporation, Korea for this study.

References

[1] Nomura T, Nishio T, Tanaka H, Mori K. Kobunshi Ronbunshu 1995; 52(2):90–6.

[2] Nomura T, Matsuda M, Nishio T, Hayashi K, Wakabayashi H, Fujita Y, Toki S. Kobunshi Ronbunshu 1998;55(8):483–9.
[3] Obata Y, Sumitomo T, Ijitsu T, Matsuda M, Nomura T. Polym Engng Sci 2001;41(3):408–16.
[4] Rybnikář F. J Appl Polym Sci 1989;38(8):1479–90.
[5] Fujiyama M, Wakino T. J Appl Polym Sci 1991;42(1):9–20.
[6] Fujiyama M, Wakino T. J Appl Polym Sci 1991;43(1):57–81.
[7] Fujiyama M. Int Polym Proc 1992;7(1):84–96.
[8] Fujiyama M, Wakino T. Int Polym Proc 1992;7(1):97–105.
[9] Fujiyama M. Int Polym Proc 1992;7(2):165–71.
[10] Fujiyama M. Int Polym Proc 1992;7(4):358–73.
[11] Alonso M, Gonzalez A, de Saja JA, Requejo A. Plast Rubber Compos Process Appl 1993;20(3):165–70.
[12] Alonso M, Velasco JI, de Saja JA. Eur Polym J 1997;33(3):255–62.
[13] Naiki M, Fukui Y, Matsumura T, Nomura T, Matsuda M. J Appl Polym Sci 2001;79(9):1693–703.
[14] Olley RH, Bassett DC. Polymer 1982;23(12):1707–10.
[15] Gedde UE. Polymer physics. London: Chapman & Hall; 1995. Chapter 9.
[16] Coulon G, Castelein G, G'Sell C. Polymer 1998;40(1):95–110.
[17] Vincent M, Agassant JF. Polym Compos 1986;7(2):76–83.
[18] Ozawa T. Polymer 1971;12(3):150–8.
[19] Liu TX, Mo ZS, Wang SG, Zhang HF. Polym Engng Sci 1997;37(3):568–75.